Franke, M. Sanchez, Z. Misulovin, M. C. Nussenzweig, *J. Exp. Med.* **175**, 1669 (1992); A. R. Venkitaraman, G. T. Williams, P. Dariavach, M. S. Neuberger, *Nature* **352**, 777 (1991).
15. G. G. Lennon and R. P. Perry, *Nature* **318**, 475 (1985); F. W. Alt, T. K. Blackwell, G. D. Yancopoulos, *Science* **238**, 1079 (1987).
16. M. S. Schlissel, L. M. Corcoran, D. Baltimore, *J. Exp. Med.* **173**, 711 (1991).
17. F. W. Alt *et al.*, *EMBO J.* **3**, 1209 (1984).
18. A. Ehlich *et al.*, *Cell* **72**, 695 (1993).
19. P. Ferrier *et al.*, *EMBO J.* **9**, 117 (1990); A. Okada, M. Mendelsohn, F. Alt, *J. Exp. Med.* **180**, 261 (1994).
20. U. Grawunder, D. Haasner, F. Melchers, *Int. Immunol.* **5**, 1609 (1993).
21. H. Karasuyama *et al.*, *Cell* **77**, 133 (1994).
22. P. J. Swiatek and T. Gridley, *Genes Dev.* **7**, 2071 (1993).
23. D. A. Melton *et al.*, *Nucleic Acids Res.* **12**, 7035 (1984).
24. A. Kudo, N. Sakaguchi, F. Melchers, *EMBO J.* **6**, 103 (1987).
25. M. S. Schlissel and D. Baltimore, *Cell* **58**, 1001 (1989); T. E. F. Costa, H. Suh, M. C. Nussenzweig, *Proc. Natl. Acad. Sci. U.S.A.* **89**, 2205 (1992).
26. H. P. Petree, F. Livak, D. Burtrum, S. Mazel, *J. Exp. Med.* **182**, 121 (1995).
27. Murine genomic Igβ DNA clones were isolated from a 129/Sv strain genomic library. The long arm of the targeting vector consisted of 10 kilobases (kb) of DNA 5′ to the Eco RV site, which is 1 kb upstream of the Igβ promoter. The short arm was a 1.2-kb fragment from the Kpn I site in the second exon to the Xba I site in the third intron. Homologous insertion resulted in a deletion of the promoter, the first exon, and the portion of the second exon that is 5′ to the Kpn I site. The targeting construct was linearized with Not I and transfected into CJ7 (*22*) embryonic stem (ES) cells. Two hundred ES cell clones were screened, and four clones carrying the mutation in Igβ were identified by Southern blotting. All four were injected into C57Bl/6 blastocysts, and three of the four clones produced chimeric mice that transmitted the mutation.
28. For Northern blotting, 2 μg of total RNA was run on denaturing formaldehyde-agarose gels and transferred to nylon membranes. Filters were probed with reverse RNA probes (*23*). Glyceraldehyde-3-phosphate dehydrogenase (GAPDH) was used as a loading control. For RT-PCR experiments, total RNA was first digested with deoxyribonuclease (DNAse) and then reverse-transcribed (*16*). Amounts of cDNA were normalized to GAPDH and λ5 (see Fig. 2). Amplification conditions were as follows: 30 cycles of 1 min at 94°C, 1 min at 60°C, and 1.75 min at 72°C, followed by a single 10-min period at 72°C. PCR products were electrophoresed on agarose gels, transferred to nylon membranes, and probed with the following specific DNA probes: (i) Hind III–Bgl I fragment from the mouse Cκ region for κ° and κ; (ii) Eco RI fragment covering mouse μCH1 for μJ558L, μ7183, Dμ, μ°, and Iμ; (iii) mouse λ5 cDNA for λ5 (*24*); and (iv) V_HJ558L for $V_H$ster. The PCR primers for μ°, Iμ, Dμ, μJ558L, μ7183, κ°, κ, λ5, and $V_H$ster were as described previously (*10, 16, 25*).
29. Lymph nodes and spleens were photographed at magnifications of ×10 and ×25, respectively. Tissues from 5-week-old mice were fixed with formalin, and tissue sections were stained with hematoxylin and eosin.
30. For two-color analysis, single-cell suspensions from lymphoid organs of 5-week-old mutant and littermate control mice were prepared for staining as described previously and analyzed on a Becton Dickinson FACScan with CELLQuest software (*6*). Bone marrow cells (yield, 1.5×10^7 to 2×10^7 cells per mouse for all strains) were stained with phycoerythrin (PE)–labeled antibody to B220 and fluorescein isothiocyanate (FITC)–labeled antibody to CD43, spleen cells (yield, 6×10^7 to 7×10^7 for $Igβ^{-/-}$ mice and 10^8 for wild-type mice) were stained with FITC-labeled antibody to μ and PE-labeled antibody to B220, and thymocytes (yield, 10^8 for both $Igβ^{-/-}$ mice and wild-type controls) were stained with PE-labeled antibody to CD4 and FITC-labeled antibody to CD8 (Pharmingen). Gating was based on lymphocyte scatter; 5000 to 10,000 gated events are shown in each panel. For four-color analysis, bone marrow cells were stained simultaneously with allophycocyanin (APC)-labeled antibody to B220, FITC-labeled antibody to CD43, PE-labeled antibody to HSA, and biotinylated antibody to BP-1. BP-1 was visualized with Texas Red avidin (Pharmingen). Gating was on lymphocyte scatter and then on $CD43^+B220^+$ cells as described (*12*). Ten thousand events taken from the $CD43^+B220^+$ gate are shown in each panel. Analysis was on a FACstar-plus system with the Lysis-II program (Becton Dickinson).
31. A. Ehlich, V. Martin, W. Muller, K. Rajewsky, *Curr. Biol.* **4**, 573 (1994).
32. For PCR, bone marrow DNA was amplified as described previously (*16, 24*). VJ558L primers were used for the heavy chain in this experiment, but similar results were also seen with V7183 primers. PCR fragments were visualized after transfer to nylon membranes by probing with an Eco RI fragment that covers the mouse J_H region (V-DJ_H and D_H-J_H). The two bands detected correspond to D_H-J_H1 and 2 and V-DJ_H1 and 2, respectively. Control primers were from the J-CH1 intervening sequence (IVS) (*24*).
33. For Southern blotting, B cells were purified from bone marrow by sorting $CD43^+B220^+$ and $CD43^+B220^-$ cells (*12*). The gates were set with *RAG-1*$^{-/-}$ $CD43^+B220^+$ control cells. The sorted cells were processed to make DNA for restriction enzyme digestion in agarose, as described (*26*). DNA samples were digested with Pst I, separated on agarose gels, transferred to nylon membranes, and probed with a combination of a 700–base pair Pst I–Pst I probe from the 5′ end of D_H (*17*) and a 650-bp Hind III–Pst I fragment that covers Igμ-CH4.
34. We thank M. Sanchez and T. Dlohery for the FACS analyses; K. Sokol for histology; H. Petree, A. Fienberg, X. Qin, and Z. Misulovin for technical advice; and S. Gezelter and F. Isdell for cell sorting.

13 October 1995; accepted 7 February 1996

Homocysteine Antagonism of Nitric Oxide–Related Cytostasis in *Salmonella typhimurium*

Mary Ann De Groote, Traci Testerman, Yisheng Xu, George Stauffer, Ferric C. Fang*

Nitric oxide (NO) is associated with broad-spectrum antimicrobial activity of particular importance in infections caused by intracellular pathogens. An insertion mutation in the *metL* gene of *Salmonella typhimurium* conferred specific hypersusceptibility to *S*-nitrosothiol NO-donor compounds and attenuated virulence of the organism in mice. The *metL* gene product catalyzes two proximal metabolic steps required for homocysteine biosynthesis. *S*-Nitrosothiol resistance was restored by exogenous homocysteine or introduction of the *metL* gene on a plasmid. Measurement of expression of the homocysteine-sensitive *metH* gene indicated that *S*-nitrosothiols may directly deplete intracellular homocysteine. Homocysteine may act as an endogenous NO antagonist in diverse processes including infection, atherosclerosis, and neurologic disease.

Nitric oxide has antimicrobial activity against a broad array of pathogens ranging from viruses to helminths (*1*), but the specific reactive nitrogen intermediates responsible for this activity are undetermined. *S*-Nitrosothiols such as *S*-nitrosoglutathione (GSNO) are candidate endogenous antimicrobial mediators because they have broad-spectrum microbiostatic activity (*2, 3*) and have been detected during inflammatory states in vivo (*4*). Although *S*-nitrosothiols can function as $NO^·$ donors, observations in the Gram-negative bacterium *Salmonella typhimurium* suggest that their cytostatic activity actually results from NO^+ (nitrosonium) transfer after active transport of the *S*-nitrosothiol into the target cell (*2*). *Salmonella* provides a model system in which to examine the antimicrobial properties of NO because it is genetically well characterized (*5*), resides principally within host cells (*6*), and requires host expression of NO-stimulatory cytokines for effective clearance (*7*).

A *S. typhimurium* MudJ (*8*) transposon library was enriched for mutants hypersusceptible to *S*-nitrosothiols by simultaneous exposure to cycloserine and subinhibitory concentrations of GSNO (*9*). A clone highly susceptible to GSNO and other nitrosothiols was found to harbor an insertion in the *metL* gene (*10*), encoding the bifunctional enzyme aspartokinase II–homoserine dehydrogenase II (AKII-HDII). The *metL* mutant strain was designated *S. typhimurium* MF1000. AKII-HDII catalyzes two independent proximal steps in the prokaryotic biosynthetic pathways that convert aspartate to lysine, threonine, and methionine (Fig. 1). The increased susceptibility conferred by the *metL* mutation appears to be specific for *S*-nitrosothiols, because no marked effect on susceptibility to the per-

M. A. De Groote, T. Testerman, Y. Xu, F. C. Fang, Departments of Medicine, Pathology, and Microbiology, University of Colorado Health Sciences Center, Denver, CO 80262, USA.
G. Stauffer, Department of Microbiology, University of Iowa, Iowa City, IA 52242, USA.
*To whom correspondence should be addressed.

oxynitrite donor SIN-1 (3-morpholinosydnonimine hydrochloride), the NO· donor DETA-NO (diethylenetriamine-NO adduct), hydrogen peroxide (H_2O_2), or the $O_2^{\cdot-}$-generating redox-cycling agent paraquat (methyl viologen) was evident when assayed by a disk diffusion method (Fig. 2A).

Transduction of the *metL*::MudJ insertion into wild-type *S. typhimurium* conferred S-nitrosothiol hypersusceptibility. The *Escherichia coli metL* gene was cloned (*11*) and reintroduced on a plasmid; it restored GSNO resistance (*12*). The addition of 1 mM homocysteine, homoserine, or methionine abrogated GSNO-mediated cytostasis in both *metL* mutant and wild-type *S. typhimurium*, but the addition of diaminopimelate or threonine did not, suggesting that it is the homocysteine-methionine arm of the aspartate metabolic pathway that is specifically involved in the mechanism of S-nitrosothiol resistance.

Salmonella typhimurium carrying a *metL* mutation was not auxotrophic for methionine because of the presence of a related enzyme (AKI-HDI) encoded by the *thrA* gene (*13*). The *thrA* mutant *S. typhimurium* SA2824 was also hypersusceptible to S-nitrosothiols (Fig. 2B). A mutation in *metJ*, which encodes an aporepressor of homocysteine and methionine synthetic enzymes (*14*), conferred decreased GSNO susceptibility compared to wild-type strains. In contrast, a mutation in *metK*, which encodes S-adenosylmethionine synthetase, conferred increased GSNO susceptibility despite effects of this mutation similar to those of *metJ* on methionine biosynthetic gene regulation (*15*). These observations can be explained by the role of the *metK* gene product in regenerating homocysteine from methionine (Fig. 1); intracellular concentrations of homocysteine are likely to be increased in a *metJ* mutant as a result of increased synthetic activity, but decreased in a *metK* mutant because of deficiency in the salvage pathway.

Collectively, these data suggest that homocysteine, the only thiol intermediate in the *Salmonella* methionine biosynthetic pathway, can function as an endogenous NO antagonist. Transfer of NO^+ from S-nitrosothiols to the sulfhydryl center of homocysteine may redirect NO away from other cellular targets. Resistance to S-nitrosothiol–mediated cytostasis is directly proportional to predicted homocysteine concentrations.

If S-nitrosothiols and homocysteine interact directly, exposure to S-nitrosothiol would be predicted to deplete the intracellular homocysteine pool. Because it has not been possible to measure intracellular homocysteine concentrations in bacteria by direct methods, a homocysteine-sensitive reporter gene fusion was used as an indicator of relative amounts of homocysteine. The *metH* gene is negatively regulated by homocysteine (*16*). A plasmid containing a *metH::lacZ* transcriptional fusion (*17*) was introduced into wild-type *S. typhimurium* 14028s and the isogenic *metL* derivative MF1000. Expression of *metH* measured as β-galactosidase activity was increased in a *metL* mutant (Fig. 3A), probably reflecting reduced homocysteine production. Exposure of the wild-type strain carrying the *metH::lacZ* fusion to 1 mM GSNO mimicked the effects of the *metL* mutation (Fig.

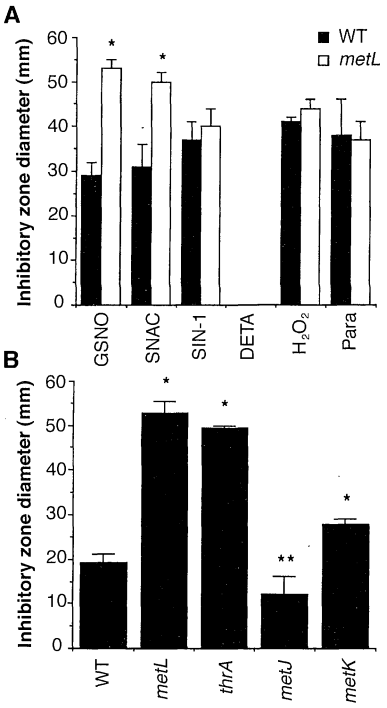

Fig. 2. Disk diffusion susceptibility assays. (**A**) Susceptibility of *metL S. typhimurium* to reactive nitrogen and oxygen intermediates. Susceptibility was measured by the Bauer-Kirby disk diffusion method (*2, 23*); zone diameter is proportional to susceptibility. Fifteen microliters of a NO-donor compound [500 mM GSNO, *S*-nitroso-*N*-acetylcysteine (SNAC), SIN-1, or DETA-NO (DETA)], 3% H_2O_2, or 1.9% paraquat (Para) were added to a 0.64-cm paper disk placed over a lawn of 10^6 bacteria spread in a 100-μl volume onto M9 minimal agar with 0.2% glucose. The resulting zone of inhibition was measured after overnight incubation at 37°C. Susceptibility of wild-type (solid bars) and *metL* (open bars) strains were compared. Error bars, SDM. $^*P < 0.01$ by Student's *t* test adjusted for multiple comparisons. (**B**) Correlation between homocysteine and GSNO resistance. GSNO susceptibility was determined as in (A). Details of strain construction are as described (*15*). The *metL* gene encodes aspartokinase II–homoserine dehydrogenase II, *thrA* encodes aspartokinase I–homoserine dehydrogenase I, *metJ* encodes an aporepressor of homocysteine and methionine biosynthetic genes, and *metK* encodes *S*-adenosylmethionine synthetase. Error bars, SDM. $^*P < 0.01$; $^{**}P < 0.05$ by Student's *t* test adjusted for multiple comparisons.

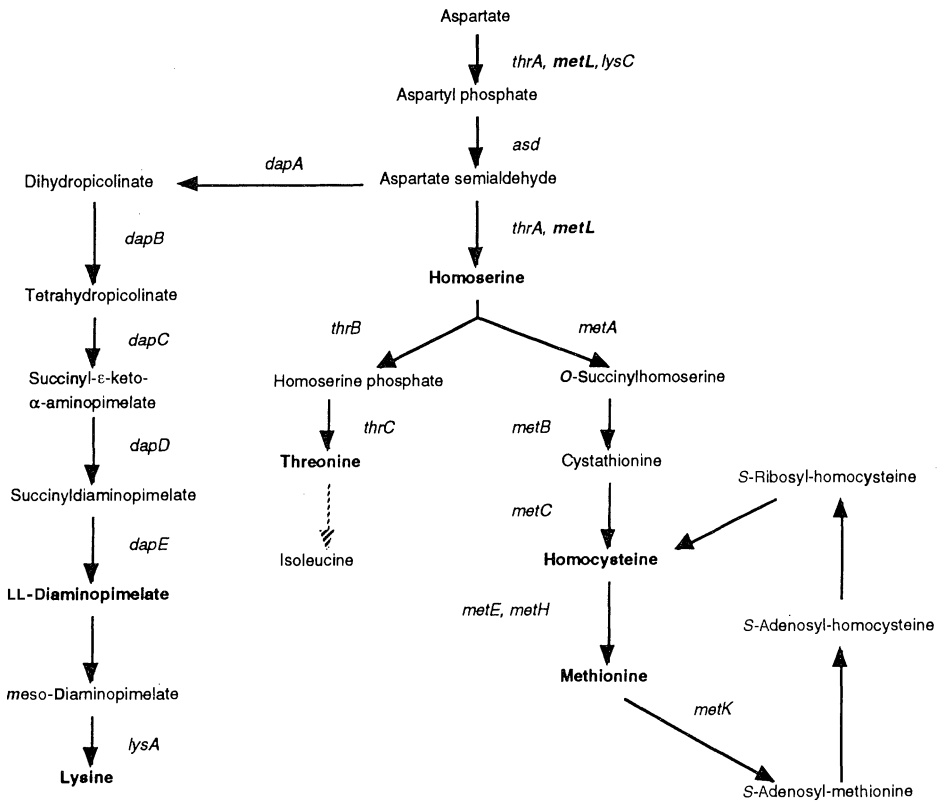

Fig. 1. Biosynthesis of lysine, threonine, and methionine in *S. typhimurium*. Genes whose products catalyze specific enzymatic steps are denoted in italics.

3B), whereas a control *neo::lacZ* fusion was unaffected by GSNO, providing evidence of a specific GSNO-homocysteine interaction that depletes homocysteine.

We investigated the relevance of *S*-nitrosothiol antagonism by homocysteine in vitro to antimicrobial host defenses in vivo. *Salmonella typhimurium* carrying a *metL* mutation was highly attenuated for virulence in C3H/HeN mice (*Ity*^{r} *Lps*^{n}) after intraperitoneal administration (Fig. 4). In contrast, the *metL* mutation had little effect on *Salmonella* virulence in BALB/c (*Ity*^{s} *Lps*^{n}) mice (*12*). Because the *Ity*^{r} genotype is associated with higher inducible NO synthase activity early in the course of infection (*18*), the differences in murine strain susceptibility are consistent with a direct correlation between the in vitro susceptibility of *metL S. typhimurium* to *S*-nitrosothiols and in vivo susceptibility to NO-dependent antimicrobial mechanisms. Moreover, inhibition of NO synthesis by aminoguanidine restored the virulence of *metL S. typhimurium* to wild-type levels in *Ity*^{r} mice (Fig. 4). Persisting differences in the virulence of *metL* and wild-type *S. typhimurium* in the presence of aminoguanidine suggest that aminoguanidine did not completely inhibit NO production in these experiments or that the *metL* mutant is less virulent for reasons related to both NO-dependent and NO-independent mechanisms.

The central importance of homocysteine is further reinforced by the observation that *metB* mutant *S. typhimurium* (which is unable to produce either homocysteine or methionine) was highly attenuated for virulence in C3H/HeN mice, whereas otherwise isogenic *metE S. typhimurium* remained fully virulent despite its methionine auxotrophy (*19*). Thus, GSNO or related species apparently have an important role as antimicrobial mediators in salmonellosis, and microbial homocysteine production is a determinant of *Salmonella* virulence and resistance to *S*-nitrosothiols.

Accumulating evidence strongly implicates homocysteine as an independent risk factor in the development of vascular and neurologic disease, although the pathogenic mechanism is unknown (*20*). The vasodilatory, antiplatelet, antioxidant, antiproliferative, and neuroregulatory actions of *S*-nitrosothiols are the opposite of those attributed to homocysteine (*21*). A biochemical interaction between *S*-nitrosothiols and homocysteine may be a central mechanistic feature in such diverse biological processes as infection, neoplasia, neurologic disease, and atherosclerosis.

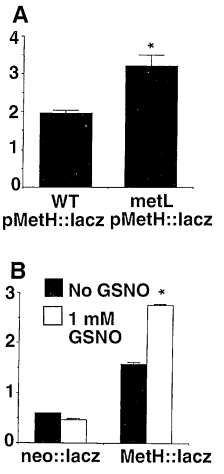

Fig. 3. β-Galactosidase assays. (**A**) Expression of *metH::lacZ* in wild-type and *metL* mutant *S. typhimurium*. β-Galactosidase assays were performed on overnight cultures as described (*24*). Construction of a plasmid carrying a *metH::lacZ* transcriptional fusion is detailed in (*17*). Error bars, SDM. *$P < 0.01$ by Student's *t* test. (**B**) Expression of *metH::lacZ* after exposure to GSNO. β-Galactosidase assays were performed on wild-type *S. typhimurium* 14028s carrying the *metH::lacZ* plasmid or the control *neo::lacZ* plasmid (*25*). Cells in mid-logarithmic growth were exposed to GSNO (0 or 1.0 mM), and β-galactosidase activity was measured 8 hours later. Error bars, SDM. *$P < 0.01$ by Student's *t* test adjusted for multiple comparisons.

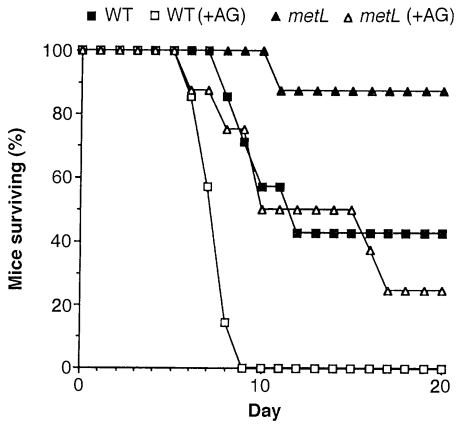

Fig. 4. Virulence of *metL* and wild-type *S. typhimurium* in C3H/HeN mice. *Salmonella typhimurium* 14028s (wild type) or MF1000 (*metL*) (1 × 10^3 to 2 × 10^3 organisms) were inoculated intraperitoneally into 6-week-old female C3H/HeN mice (*Ity*^{r} *Lps*^{n}; Jackson Laboratories, Bar Harbor, Maine). Additional groups of mice were administered 2.5% aminoguanidine (AG) (*26*) in their drinking water beginning 7 days before inoculation. No mortality occurred in control animals receiving intraperitoneal phosphate-buffered saline or oral aminoguanidine alone during the 21-day experiments. *metL* and wild-type *S. typhimurium* were administered to BALB/c mice (*Ity*^{s} *Lps*^{n}) with little apparent difference in virulence (*12, 18*). All mice that received 2 × 10^3 intraperitoneal organisms were dead within 10 days.

REFERENCES AND NOTES

1. M. A. De Groote and F. C. Fang, *Clin. Infect. Dis.* **21**, S162 (1995).
2. M. A. De Groote *et al.*, *Proc. Natl. Acad. Sci. U.S.A.* **92**, 6399 (1995).
3. K. A. Rockett, M. M. Awburn, W. B. Cowden, I. A. Clarke, *Infect. Immun.* **59**, 3280 (1991).
4. B. J. Gaston *et al.*, *Proc. Natl. Acad. Sci. U.S.A.* **90**, 10957 (1993).
5. K. E. Sanderson, A. Hessel, K. E. Rudd, *Microbiol. Rev.* **59**, 241 (1995).
6. B. B. Finlay and S. Falkow, *Mol. Microbiol.* **3**, 1833 (1989).
7. C. Nauciel and F. Espinass-Maes, *Infect. Immun.* **60**, 450 (1992).
8. B. A. Castilho, P. Olfson, M. J. Casadaban, *J. Bacteriol.* **158**, 488 (1984).
9. A *S. typhimurium* 14028s MudJ transposon library containing ~50,000 independent insertions was constructed by use of *S. typhimurium* TT10388, as reported [K. Hughes and J. M. Roth, *Genetics* **119**, 9 (1988)]. The library was subcultured in M9 medium. GSNO was added to logarithmically dividing cells at a final concentration of 2 mM (which is not inhibitory for rapidly dividing cells). One hour later, cycloserine was added to a final concentration of 100 mg/liter. Cycloserine is specifically bactericidal for dividing cells, as described [F. Bolivar, R. L. Rodriguez, M. C. Betlach, H. W. Boyer, *Gene* **2**, 75 (1977)]. Therefore, this protocol provides a positive selection for mutants with enhanced GSNO susceptibility. After 1 hour of exposure to cycloserine, the cells were washed, allowed to enter stationary phase, diluted into fresh medium, and enriched for a second time.
10. After enrichment, the library was plated as individual colonies that were screened for GSNO susceptibility. Seven clones with highly increased susceptibility to GSNO were identified. The attL-junction fragments were cloned and sequenced as described (*2*). All seven clones were shown to have identical insertions between nucleotides 325 and 326 of the *S. typhimurium metL* gene. The sequenced region was shown to be 80% identical at the nucleotide level and >90% identical at the amino acid level to the corresponding region of *E. coli metL* (*22*). We used bacteriophage P22 to transduce the *metL*::MudJ insertion into a new wild-type background; 100% cotransduction of GSNO hypersusceptibility was confirmed.
11. Oligonucleotide primers 5′-AAGCTTGGAGGGTAAAAATGAGTGTGAGTGTGATTGCGCAGG-3′ and 5′-GGATCCCCGGGCATTATTAAATTTCTGAAATTACAA-3′ were used to amplify the *E. coli metL* gene (*22*) from DH5α genomic DNA in a polymerase chain reaction (PCR). The first primer incorporates a ribosomal binding sequence to allow *metL* expression; the native *metL* gene is ordinarily expressed as part of the *metBL* operon. The 2.4-kb PCR product was cloned into pBLUESCRIPT (Stratagene) and introduced into *metL* mutant *S. typhimurium*.
12. M. A. De Groote and F. C. Fang, unpublished data.
13. M. Katinka *et al.*, *Proc. Natl. Acad. Sci. U.S.A.* **77**, 5730 (1980).
14. I. Saint-Girons, N. Duchange, G. N. Cohen, M. M. Zakin, *J. Biol. Chem.* **259**, 14282 (1984).
15. Mutant *S. typhimurium* strains SA2824 (LT2 *thrA*13), DS163 (LT2 *metJ*713), and DS1373 (LT2 *metK*36) were obtained from K. Sanderson at the *Salmonella* Genetic Stock Centre (Calgary, Alberta, Canada). *Salmonella typhimurium* LT2 was used as the wild-type control for comparative GSNO susceptibility studies with these strains. M9 medium was supplemented with 500 μM threonine for studies with *S. typhimurium* SA2824; threonine supplementation has no effect on the GSNO inhibitory zone diameter obtained for wild-type *S. typhimurium*. All GSNO susceptibility studies were done a minimum of three times. Mutations in *metJ* and *metK* both derepress methionine biosynthetic genes [J. T. Mulligan, W. Margolin, J. H. Krueger, G. C. Walker, *J. Bacteriol.* **151**, 609 (1982)].
16. M. L. Urbanowski and G. V. Stauffer, *ibid.* **171**, 3277 (1989).
17. *metH* encodes a vitamin B_{12}-dependent transmethylase. The *metH::lacZ* plasmid pGS201 carries a *metH* transcriptional fusion with *lacZYA*, as described [K. A. Byerly, M. L. Urbanowski, G. V. Stauffer, *ibid.* **173**, 3547 (1991)].
18. T. G. Evans, L. Thai, D. L. Granger, J. B. Hibbs Jr., *J. Immunol.* **151**, 907 (1993); S. Formica, T. I. A. Roach, J. M. Blackwell, *Immunology* **82**, 42 (1994); C. Nathan, *Cell* **82**, 873 (1995).
19. *metB* encodes cystathionine γ-synthase and *metE* encodes a vitamin B_{12}–independent transmethylase. Tn10 insertions in *metB* (*metB::879*) and linked to *metE* (*metE551*) were obtained from K. Sander-

son at the *Salmonella* Genetic Stock Centre (Calgary, Alberta, Canada). These were transduced with bacteriophage P22 into wild-type *S. typhimurium* 14028s; transductants were phenotypically confirmed to be methionine auxotrophs. Intraperitoneal inoculation of 1×10^4 *metB* mutant *S. typhimurium* was lethal in zero of four C3H/HeN mice (Charles River Laboratories) during a 14-day experiment and did not result in visible illness. In contrast, 5×10^3 *metE* mutant *S. typhimurium* killed two of four mice and made all of the infected mice ill.

20. K. S. McCully, *Am. J. Pathol.* **56**, 111 (1969); G. H. J. Boers, A. G. H. Smals, F. J. M. Trijberis, *N. Engl. J. Med.* **313**, 709 (1985); R. Clarke *et al.*, *ibid.* **324**, 1149 (1991); J. Selhub *et al.*, *ibid.* **332**, 286 (1995).
21. J. S. Stamler *et al.*, *J. Clin. Invest.* **91**, 308 (1993); J. Tsai *et al.*, *Proc. Natl. Acad. Sci. U.S.A.* **91**, 6369 (1994); M. J. Stampfer and M. R. Malinow, *N. Engl. J. Med.* **332**, 328 (1995).
22. M. M. Zakin, N. Duchange, P. Ferrara, G. N. Cohen, *J. Biol. Chem.* **258**, 3028 (1983).
23. A. W. Bauer and W. M. M. Kirby, *Am. J. Clin. Pathol.* **45**, 493 (1966).
24. J. H. Miller, *Experiments in Molecular Genetics* (Cold Spring Harbor Laboratory, Cold Spring Harbor, NY, 1972). Each β-galactosidase assay was performed three times.
25. pFF200 contains the neomycin gene promoter of transposon Tn5 transcriptionally fused to the *E. coli lacZ* gene on a pACYC184 replicon [A. C. Chang and S. N. Cohen, *J. Bacteriol.* **134**, 1141 (1978)].
26. Aminoguanidine is a moderately selective inhibitor of the cytokine-inducible form of NO synthase (NOS II) that can be orally administered [J. Chan, K. Tanaka, D. Carroll, J. Flynn, B. R. Bloom, *Infect. Immun.* **63**, 736 (1995)].
27. We are grateful to D. Granger, E. Groisman, and J. Stamler for helpful suggestions and to K. Sanderson and A. Hessel for gifts of bacterial strains. Supported in part by grants from the U.S. Department of Agriculture (9401954), the National Institutes of Health (AI32463), and the Thorkildsen Research Fellowship Program.

21 November 1995; accepted 27 February 1996

CNS Gene Encoding Astrotactin, Which Supports Neuronal Migration Along Glial Fibers

Chen Zheng, Nathaniel Heintz, Mary E. Hatten*

Vertebrate central nervous system (CNS) histogenesis depends on glia-guided migration of postmitotic neurons to form neuronal laminae. Previous studies have established that the neuronal protein astrotactin functions in murine cerebellar granule cell migration in vitro. The gene encoding astrotactin predicts a protein with three epidermal growth factor repeats and two fibronectin type III repeats. Astrotactin messenger RNA is expressed in postmitotic neuronal precursors in the cerebellum, hippocampus, cerebrum, and olfactory bulb, where migration establishes laminar structures. Fab fragments of antibodies to a recombinant astrotactin peptide blocked migration of cerebellar granule neurons in vitro along astroglial fibers. Transfection of astrotactin complementary DNA into 3T3 cells indicated that astrotactin acts as a ligand for neuron-glia binding during neuronal migration.

The vertebrate cortex is patterned into several layers, each with a distinctive set of neurons (*1*, *2*). Studies on the developing brain suggest that cells destined to form specific cortical layers migrate along radial glial fibers under the direction of the protein astrotactin (*3*–*5*). A set of candidate astrotactin clones was generated by screening of a P3 to P5 granule cell complementary DNA (cDNA) expression library (*6*, *7*) with a polyclonal antiserum to astrotactin that inhibits neuronal migration (*4*). Among 39 immunopositive clones examined, one clone, GC14, encoded a brain-specific transcript of about 7 kb. The open reading frame of this transcript [2500 base pairs (bp)] predicts a polypeptide of 100 to 105 kD, with four potential N-linked glycosylation sites.

The NH_2-terminus of GC14 begins with a signal peptide of 15 amino acids (Fig. 1A). The most notable feature of the deduced GC14 protein is the presence of domains homologous to several well-characterized signaling and adhesion molecules. The sequence of GC14 contains three cysteine-rich epidermal growth factor (EGF)–like repeats (*8*) and two domains with homology to a motif of 90 amino acids found in fibronectin type III (FNIII) (*9*). EGF repeats are found in the extracellular domains of several proteins (*10*, *11*) and have been implicated in intercellular signaling in neuronal development. FNIII repeats have been found in axonal glycoproteins of the immunoglobulin G (IgG) superfamily (*12*). The number and arrangement of these motifs and the absence of IgG-like domains suggest that astrotactin is unlike other cell adhesion or signaling molecules.

In a Northern (RNA) blot analysis, GC14 hybridized to a single mRNA band of about 7 kb that was expressed in the brain (specifically in the cerebellum and forebrain), but not in the kidney, heart, liver, lung, thymus, or spleen (*13*). GC14 mRNA was expressed in purified cerebellar granule cells but not in glial cells.

In the developing murine cerebellar cortex, GC14 transcripts were abundant in the deeper aspect of the external germinal layer (EGL), where cells are undergoing early steps in differentiation, as well as in migratory and postmigratory cells (Fig. 2, A through C). Glial cells, including the Bergmann glia of the molecular layer and astrocytes within the white matter, were unlabeled. Proliferating precursor cells, which occupy the superficial aspect of the EGL, did not express astrotactin mRNA or protein. Rather, expression commenced in the deeper aspect of the EGL where postmitotic precursor cells bind to astroglial fibers, extend parallel fibers, migrate along the Bergmann glial fibers, detach from the glial fibers, and move past Purkinje neurons. Astrotactin expression continued as differen-

B EGF repeats:

```
EGF1:  CSKD-NGGCSKNFRCI--------SDRKLDSTGCVCPSGLSPMKDSSGC
(328 to 367)
EGF2:  CSDGFNGGC--EQLCLQQMAPFPEDPLYNILMFCGCIEDYKLGVDGR-C
(376 to 423)
EGF3:  TQRLLQEATMSSLWC--------SGTGDVIEDWCRCDSTAFGADGLPTC
(701 to 742)
EGF-mouse: C      GC    C                  C C        G  C
```

C FNIII repeats:

```
ASTFNI:  PDFLTGMVNFSEVSGYPVLQHWKVRSVMYHIKLNQAAISQAFSNALHSLDGATSRADFVALLDQFGNHYIQEAVYGFEESCS
(511 to 593)
ASTFNII: PVLRLSTVHEP--SSNLVVLEWEHSEPPIG----VQIVDYLYRQEKVTDRMDHSKVETETV-LSFVDDIISGAKAPCAMP-S
(747 to 821)
FNIII:   P--L---------T-----V-W--P..4-8aa..I--Y-V-Y----------..5-14aa..L-P---Y---V-A------S
```

Fig. 1. Deduced amino acid structure of astrotactin and homology with known proteins. (**A**) Schematic representation of the domain structure of astrotactin. Black, signal peptide; gray, EGF-like repeat; hatched, FNIII-like repeat. (**B**) Alignment of the three EGF repeats and (**C**) alignment of the two FNIII repeats in astrotactin over the consensus of the respective motifs (*8*, *9*). Identical amino acids are shown in bold; underlined amino acids are substitutes found in FNIII repeats of other proteins at the same positions. Dashes denote gaps to optimize the alignment. ASTFN, astrotactin FNIII repeat; aa, amino acid. Numbers indicate the positions of each repeat within astrotactin cDNA.

C. Zheng and M. E. Hatten, Rockefeller University, 1230 York Avenue, New York, NY 10021–6399, USA.
N. Heintz, Howard Hughes Medical Institute, Rockefeller University, 1230 York Avenue, New York, NY 10021–6399, USA.
*To whom correspondence should be addressed.